Journal of Sustainable Metallurgy (2021) 7:1456–1468
https://doi.org/10.1007/s40831-021-00455-y

THEMATIC SECTION: MINE TAILINGS: PROBLEM OR OPPORTUNITY? TOWARDS A COMBINED REMEDIATION AND RESOURCE RECOVERY APPROACH

Characterization of Mine Waste from a Former Pb–Zn Mining Site: Reactivity of Minerals During Sequential Extractions

Valérie Cappuyns[1,2] · Van Axelle Campen[2] · Srećko Bevandić[2] · Jillian Helser[1,2] · Philippe Muchez[2]

Received: 29 April 2021 / Accepted: 20 October 2021 / Published online: 5 November 2021

Abstract
An integrated mineralogical and chemical characterization approach was applied to different types of mine waste collected from the ancient Pb–Zn mining area of Plombières. The combination of different methods to determine (pseudo-)total element concentrations, sequential extractions, and quantitative mineralogical analysis provided detailed information on the reactivity of minerals in the waste, as well as the associated metal(loid) release under different experimental conditions. Lithium borate ($LiBO_2$) fusion was not suited to determine total metal(loid) concentrations in the investigated mine waste samples, due to the incomplete dissolution of the samples, and the volatilization of As and Cd during the fusion. Because some elements were below detection limit of X-ray fluorescence spectrometry (e.g., Cd), aqua regia digestion was useful to complement the chemical sample characterization, bearing in mind that only pseudo-total concentrations could be determined. Galena (PbS) and its alteration products, cerussite and anglesite ($PbSO_4$), were the main lead minerals associated with the mining waste. Because of the high cerussite ($PbCO_3$) content of the investigated samples (2–5 wt%), Pb not only shows the highest potential for recovery from the mining waste, but it also poses the highest environmental and human health risk. Zinc minerals showed a lower reactivity towards the BCR sequential extraction (sphalerite, ZnS) or were less abundant (willemite, Zn_2SiO_4). Quantitative XRD analysis allowed for better evaluation of the incomplete dissolution of some minerals, improving the interpretation of the sequential extraction results.

The contributing editor for this article was Stephan Pfister.

✉ Valérie Cappuyns
valerie.cappuyns@kuleuven.be

[1] KU Leuven, Center for Economics and Corporate Sustainability (CEDON), 1000 Brussels, Belgium

[2] KU Leuven, Department of Earth and Environmental Sciences, 3001 Leuven, Belgium

Graphical Abstract

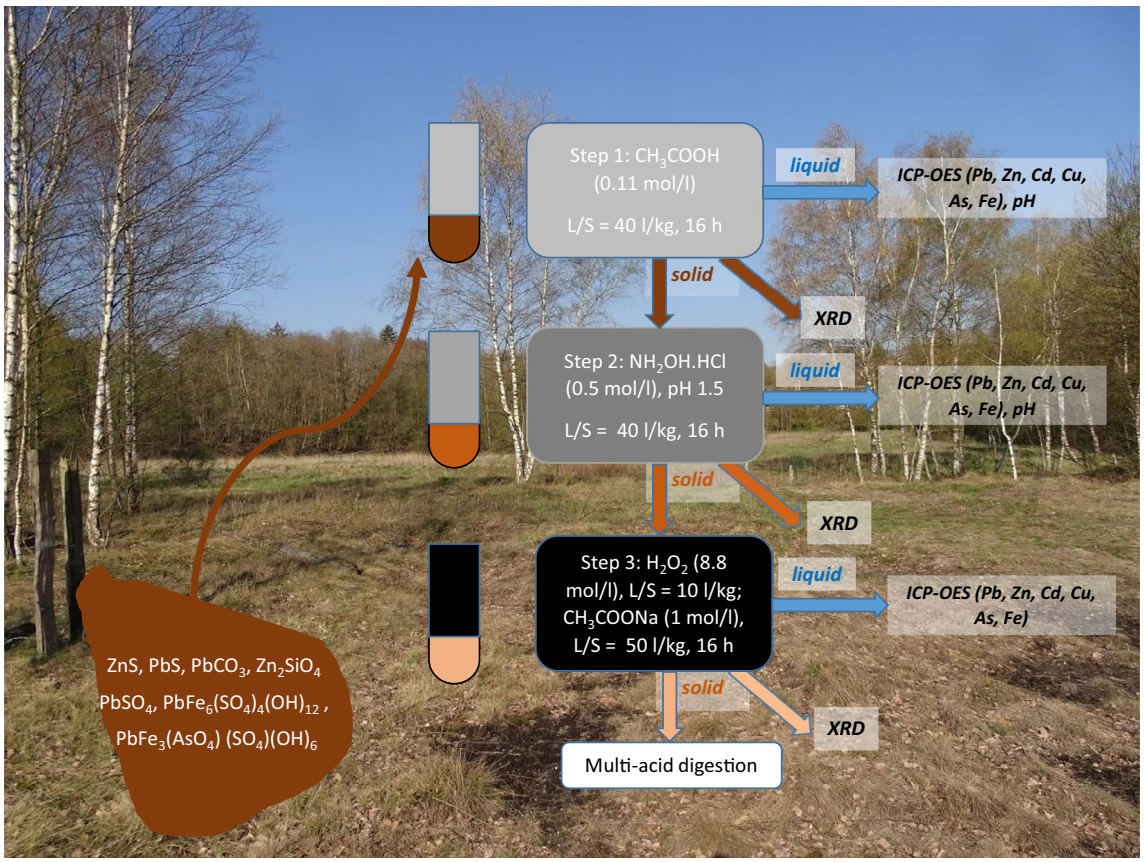

Keywords Cerussite · Leaching · Mineralogy · Sequential extractions

Introduction

Waste from extraction and processing of mineral resources represents one of the largest waste streams in the European Union (EU-27), contributing to 26.2% of the total waste generation in 2018 [1]. Pb–Zn mines occur all over the World, and it is estimated that 240 Pb–Zn mines are still active [2, 3]. Since the beginning of Pb–Zn mining in Roman times, many mines have been abandoned, leaving behind numerous sites covered with mining waste [4]. An overview of different studies dealing with geology and mining of Pb–Zn mineral deposits can be found in [2].

Each of the ore-mining and processing steps can generate mining waste with different physical and chemical properties, with associated environmental impacts, such as the generation of acid or alkaline drainage, and an increase in the chemical availability of metal(loid)s [5, 6]. Mining practice has considerably evolved over the last decades, and mining companies, nowadays, are subjected to strict regulations in order to protect human and environmental health. Abandoned sites, however, represent a serious hazard to environmental and human health if they are not managed properly [7].

The different types of waste materials encountered at mining sites not only present an environmental/human health risk, they can also be considered a potential resource. Metals as well as residual mineral fractions can be extracted from the waste, and replace primary raw materials in multiple applications. Different types of waste materials are usually found at mining sites, generally characterized by a complex composition, whose chemical and mineralogical characterization can be very challenging. The thorough characterization of these materials is essential to evaluate their environmental impact, as well as their potential for metal recovery or other beneficial applications.

Sequential extractions (SE) provide an operationally defined fractionation of elements, which is difficult to link to the solid-phase speciation of metal(loid)s or to the potential risk for human health and environment.

Commonly reported artifacts of SE are the lack of selectivity of the reagents used in the different extraction steps [8], the re-adsorption of solubilized ions by the soil matrix, and the precipitation of elements [9]. Moreover, numerous different extraction procedures have been developed during the last 50 years, making the comparison between different procedures difficult. Despite the issues mentioned above, SE can offer a better insight in the composition of waste materials, especially in combination with other techniques for material characterization, such as microscopy, X-ray diffraction (XRD) analysis, or field emission gun electron probe microanalysis (FEG-EPMA) [10].

Supplementary Table S-1 provides an overview of studies in which different types of mine and metallurgical waste were investigated with SE. The BCR (Bureau Communautaire de Référence, Community Bureau of Reference in English) SE procedure is the most frequently used procedure for mining and metallurgical waste, despite the fact that has originally been developed for sediments. The first studies in which mine waste was investigated with SE were rather speculative, merely guessing about possible mineralogical associations of elements (e.g., [11]). Over the last 20 years, XRD analysis was more frequently combined with the results of SE, providing the (*qualitative*) mineralogical composition of samples after subsequent extraction steps (e.g., [10, 12]). We are aware of one study [13], applying SE on 'special clays,' in combination with *quantitative* XRD, demonstrating the reactivity of silicate clays during SE.

This work is part of the ETN-SULTAN Project (European Training Network for the Remediation and Reprocessing of Sulfidic Mining Waste Sites) and focuses on the characterization of Pb/Zn mining waste, providing essential information to assess the resource potential, possible applications and environmental impact of the mine waste. The main objective of this study is to characterize mining waste by using sequential extractions, while gaining a more detailed understanding of the processes occurring during the different steps of the SE procedure. The present study is the first study on mine waste (which will be used as a common term to refer to mine and metallurgical waste) using quantitative XRD, not only to identify, but also quantify the minerals that remain after each step of the BCR SE. Different types of mine waste collected at the ancient Pb–Zn mining area of Plombières were investigated, using an integrated mineralogical and chemical approach. Several methods for the determination of (pseudo-)total element concentrations, SE, and mineralogical analyses were combined for a thorough characterization of the materials, as an essential contribution to evaluate the valorization potential and to assess the human health and environmental risks of the mine waste.

Methodology

Study Area

Plombières is situated in the south-eastern part of Belgium, in the area of the Verviers synclinorium, close to the tripoint of Belgium, the Netherlands, and Germany (Supplementary material, Fig. S-1). In this area, approximately 30 mines have been active from the Middle Ages until the twentieth century. In 1884, all mining activities were stopped, the mines were abandoned, but the metallurgic plant remained operational for the processing of imported ores until 1922. Besides Zn and Pb, the imported ores, mostly from Spain and Greece, also contained, among others, As, Sb, Cd, and Hg. When all mining-related activities ceased in 1922, furnaces, shafts, and other related buildings gradually disappeared from the scene [14]. The ore mineralization in Plombières not only is dominated by the sulfide minerals sphalerite (ZnS) and galena (PbS) but also contains some pyrite (FeS_2) and marcasite (FeS_2). Due to weathering at the surface the ores oxidized to secondary ore bodies consisting of carbonates, oxides, and silicates. The most frequently occurring secondary ores are calamines (a combination of smithsonite ($ZnCO_3$), hemimorphite ($Zn_4(Si_2O_7)(OH)_2{\cdot}H_2O$), and willemite ($Zn_2SiO_4$)), but traces of cerussite ($PbCO_3$), limonite ($FeO(OH){\cdot}nH_2O$), and siderite ($FeCO_3$) are found as well [15]. The most common gangue minerals include calcite, dolomite, quartz, and different phyllosilicates (e.g., muscovite, kaolinite) [16].

Today, the mining area of Plombières is a public nature reserve. The waste heaps are uncovered or covered with a small soil layer and some sparse vegetation. The mine waste is likely to pose environmental and human health risks due to the highly mobile levels of hazardous metal(loid)s [17].

Sampling

The samples used in the present study were collected from the ancient mining site in Plombières in September 2018 (Figs. S1–S6, Supplementary material). What used to be the mechanical preparation and sedimentation basin is nowadays a humid zone where nettles and some birch trees grow. Approximately every 10 m, depending on the accessibility of the area, a pit was dug with a spade and an auger to a maximum depth of 2 m, and sixty-five samples (approximately 1 kg each) were taken at different depths from 37 pits, depending on variations in color and grain size. Samples were dried in an oven at 30 °C. Part of each sample was disaggregated in a porcelain mortar and sieved

(< 180 µm). Finally, 4 samples with an interesting mineralogical composition (determined with XRD, see 2.4), were selected for further investigation. The selected waste samples, which all will be called 'mine waste,' contained very fine slag particles and brick fragments from the processing plant, and were characterized by different colors (PL_1: dark gray, PL_2: reddish gray, PL_3: brown, PL_4: light gray).

Chemical Sample Characterization

For the determination of the elemental composition of the samples, two different methods were used: XRF (X-ray fluorescence spectrometry) and lithium borate ($LiBO_2$) fusion followed by inductively coupled plasma-optical emission spectrometry (ICP-OES) analysis. XRF analyses (XRF, Panalytical Axios-Minerals, using superQ software with Omnian module) were performed using beads prepared with $C_6H_8O_7$ and LiBr solutions. For the $LiBO_2$ fusion, the sample was dissolved in a molten flux at a temperature of approximately 1050 °C, until the lithium borate melted and dissolved the sample to form a homogenous mass, which was dissolved in acid (HNO_3, 0.42 mol/l) for analysis. A detailed description of the method is provided in [18]. Reference materials GBW 7411 and SRM 2710 were also included in the $LiBO_2$ fusion method (Supplementary Table S-2).

The pH of the samples was measured in a suspension of 1 g of sample in 10 ml of water, with a Hamilton Single Pore Glass pH-electrode.

Mineralogical Sample Composition

Before XRD measurement, 1.8 g of sample was mixed with 0.2 g of internal standard. Zincite was used as an internal standard, except for the residues of the first step of the BCR SE, where rutile was used instead of zincite. The sample was then homogenized, mixed with ethanol, milled in a McCrone micronizing mill, and dried. The resulting powder (< 64 µm) was put into a powder mount for measurement. A Philips PW 1380 diffractometer was used (45 kV, 30 mA, CuKα radiation, graphite monochromator, 1 mm slit width) in a continuous scanning mode (2θ range from 5° to 65° with a step size of 0.02° and a counting time of 2 s). Mineral phases were identified with the Profex 4.0 software, using the Rietveld refinement method for quantification [19]. To exclude the presence of zincite in the samples, some samples were also measured without adding zincite.

Sequential Extractions

Sequential extractions (SE) were applied to evaluate the fractionation of metal(loid)s in the mine waste materials. The BCR extraction scheme, developed within the Standards, Measurements and Testing Programme of the EU (formerly BCR, Community Bureau of Reference) and described by [15] was followed. In summary, it consists of 3 different extraction steps, each representing different environmental conditions for metal release (Step 1: acetic acid (CH_3COOH), 0.11 mol/l; Step 2: hydroxylamine hydrochloride (NH_2OHCl), 0.5 mol/l; Step 3: hydrogen peroxide (8.8 mol/l) (twice), ammonium acetate CH_3COONa), 1.0 mol/l).

After the first two extraction steps, the pH of the solutions was measured. The mineralogical composition of the samples after each extraction step was determined by XRD. Therefore, for each sample, the extractions were performed on 4 replicates, and after each extraction step, one solid residue from each sample was put aside for mineralogical analysis. Additionally, the solid residue remaining after the third extraction step was dried and digested according to the multi-acid digestion procedure as described in [20]. The solutions obtained in the different steps were kept in a fridge (4 °C) until analysis, which was performed within 2 days after the last extraction step. The solutions were analyzed with ICP-OES (Varian 730 ES). The repeatability of the measurement was analyzed by including a blank and a mixed sample every 10 samples. The coefficient of variance of these replicates gave good results (< 10%) for all measured elements, indicating a strong reproducibility of the results. A reference material, SRM 2710, was included in the procedure to verify the quality of the analytical data (Supplementary Table S-3).

Results and Discussion

Mineralogical and Chemical Sample Composition

The mineralogical composition of the samples is represented in Table 1. The samples were characterized by a high content of amorphous phases (14–42 wt%), while the dominant minerals in all the samples were quartz (25–46%), mica's (4–16%), and feldspars (6–7% in samples PL_1 and PL_3, respectively). Sample PL_3 contained 20 wt% of goethite (FeOOH), and magnetite (Fe_3O_4) was also found in samples PL_1 and PL_3 (4 and 8% resp.). A detailed XRD and scanning electron microscopy (SEM–EDX) investigation of 40 representative samples from the same site showed that, based on the morphology and textures observed by SEM, these amorphous phase is smelting slag [21], a by-product of the pyrometallurgical processing of the ores. Samples PL_1 and PL_3 also contained a small amount (1–2 wt%) of mullite ($3Al_2O_32SiO_2$), an aluminosilicate mineral formed upon firing of aluminosilicate raw materials. It is the most important constituent of aluminosilicate ceramics

Table 1 Quantitative mineralogical composition (wt%) of the original samples (O) and after the different steps (#1, #2, #3) of the BCR SE procedure

	PL_1		PL_2				PL_3				PL_4		
	O	# 1	O	# 1	# 2	# 3	O	# 1	# 2	# 3	O	# 1	# 2
Amorphous phases	42	52.4	13.9	17.5	7.1		26.4	49.4	24.8	13.8	40.4	42.1	35.1
Quartz	29	30.6	46.4	44.3	51.9	51.5	25.2	21.4	30.1	26.6	26.1	24.5	29
Cristobalite	1	1.9									0.6	2.8	1.7
Clay minerals	2	3.4	2.2	2.1	2		2.9	3.3					
Micas	6	6.5	16.4	24.4	29.6	38.8	7.3	5.2	7.8	30.7	3.9	5.2	4.5
Mullite	2						1	2.5					
Sphalerite			10.8	7.8	8.8	1.8					2.1	2	
Willemite	1										1	0.8	
Cerussite	3		4.8				1.6				5.1		0.5
Galena	0.6	0.6	1.7	0.5	0.4	0.4	1.6	1.8	1.9	1.2	0.5	0.5	0.5
Anglesite			3.8	3.3		7.5							
Beudantite											13.2	12.8	13.4
Plumbojarosite											3.9	6.3	13.1
Goethite							20	13.2	25.5	20.1			
Magnetite	4	2.9					7.9	4.6	9.7	7.6			
Hematite	2	1.5									3.2	2.1	2.2

and refractory materials [22]. The primary Pb- and Zn-bearing minerals, related to the ores that were mined, identified are sphalerite (ZnS) (PL_2, PL_4) and galena (PbS) (all samples), as well as secondary minerals, such as willemite (Zn_2SiO_4) (PL_1, PL_4), cerussite ($PbCO_3$) (all samples), anglesite ($PbSO_4$) (PL_2), plumbojarosite ($PbFe_6(SO_4)_4(OH)_{12}$), and beudantite ($PbFe_3(AsO_4)\ SO_4)\ (OH)_6$) (PL_4). During progressive weathering of galena, cerussite or anglesite forms, depending mainly on the pH value [23, 24]. The primary PbS is often coated with these alteration products [25]. Sulfate minerals (i.e., anglesite) often occur in mine waste as the result of wet-dry processes [26]. Willemite is typically found in oxidized zinc ores and products of metallurgical extraction [27]. Beudantite forms in oxidizing, acidic conditions in a wide variety of environments. In mining environments, the occurrence of beudantite has been shown in gossan, the products of intense oxidation of massive sulfide deposits exposed at the surface [28], mine tailings [29], and acid sulfate soils [30]. The formation of beudantite also offers a mechanism for the entrapment of arsenate and lead upon oxidation of sulfidic deposits [31].

Besides the mining of galena and sphalerite, pyrite was also mined at Plombières but in lower volumes [14]. Although no pyrite was found in the samples, goethite, an oxidation product of pyrite, was found in sample PL_3.

For the determination of (pseudo-)total element composition, two methods were used: a $LiBO_2$ fusion method (followed by element analysis by ICP-OES), as well as a non-destructive determination with XRF (Supplementary Table S-4). Moreover, the results from the Aqua Regia (AR) digestion for the same 4 samples are available from [32] for comparison (Supplementary Table S-5).

Since the $LiBO_2$ fusion method was not able to completely dissolve the samples, the results are referred to as 'pseudo-total' concentrations, and the discussion is limited to Pb, Zn, Cd, As, and Fe. In comparison with the total element content determined by XRF, Pb and Zn concentrations determined by the $LiBO_2$ method are sometimes greatly underestimated (Fig. 1). The higher recovery of Zn and Fe in samples PL_2 and PL_4 by the $LiBO_2$ method, compared to the XRF determination, is probably due to sample heterogeneity. Despite the careful preparation of the samples, small metal(loid)-bearing particles can result in a heterogeneous chemical composition. A disadvantage of the $LiBO_2$ fusion method is the heating of the samples until nearly 1000 °C, which results in the loss of some elements. H_2O, CO_2, SO_2, and NO_2 are lost during heating, as well as elements that might be partially volatile because their boiling temperature is below 1000 °C ([33]; e.g., As: 613 °C, Cd: 765 °C, Zn: 907 °C). The XRF method allows for the determination of the total elemental concentrations, but a disadvantage is that the limit of quantification is higher than with the $LiBO_2$ method.

Concentrations of Zn, Cd, Pb, Fe, Cu, and As were also compared with the results of the Aqua Regia dissolution method (Fig. 2). Aqua regia (AR) consists of concentrated HNO_3 and HCl (1:3). HNO_3 is used for the primary decomposition and will mostly dissolve organic matter and several minerals, mostly sulfides and phosphates. HCl reacts with a wide range of compounds, i.e., many carbonates, oxides, hydroxides, phosphates, borates, and

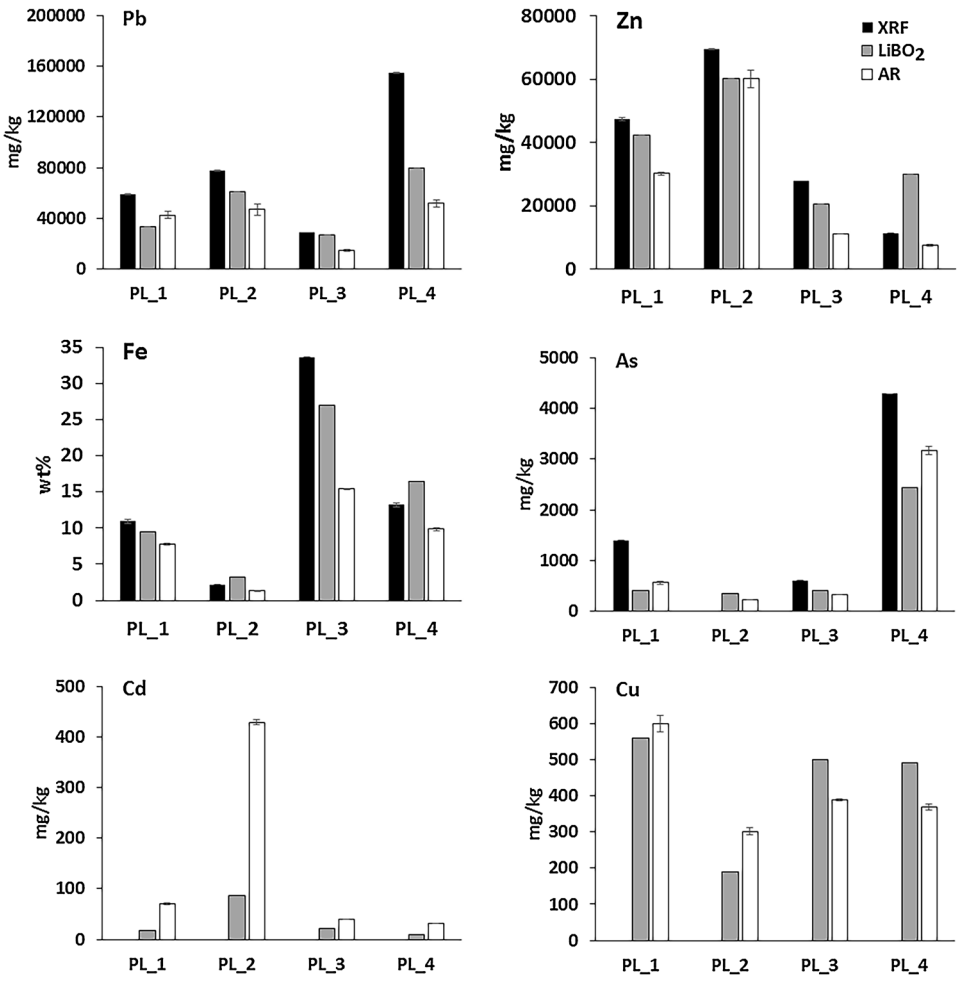

Fig. 1 (Pseudo-)total concentrations of Pb, Zn, Fe, As, Cd, and Cu determined with different methods

sulfides. Fe-minerals, such as goethite and ferrihydrite, can act as sinks for metal(loid)s and are most likely dissolved by the acid digestion. Refractory Fe-minerals in the slags, however, are not dissolved by the AR digestion. The insoluble residue remaining after AR digestion amounted to, respectively, 61, 72, 36, and 57 wt% in samples PL_1, PL_2, PL_3, and PL_4 and mainly consisted of amorphous phases, silicates, clay minerals, and feldspars [32] In sample PL_2, cottunite ($PbCl_2$) was found in the residue after AR digestion of samples PL_2 and PL_4, indicating that some Pb that was initially dissolved, precipitated again during the AR digestion.

Despite the incomplete sample dissolution with AR, higher Cd and As concentrations were found than with the $LiBO_2$ method, which is explained by the volatilization of Cd and As during the $LiBO_2$ fusion. Moreover, Cd concentrations were below the detection limit of the XRF method, which shows the importance of combining different analytical methods for the chemical characterization of these types of samples. For Cu, with a boiling point of 2868 °C [33], the results of the $LiBO_2$ and AR method are similar (Fig. 1). Arsenic was detected by XRF, except in sample PL_2, which also did not release significant amounts of As during AR digestion.

Overall, elevated concentrations of Pb (up to 15 wt%) or Zn (up to 6 wt%) are in accordance with the occurrence of Pb/Zn-bearing minerals. The mine waste samples also contain significant amounts of As (221–3173 mg/kg), Cu (301–599 mg/kg), and Cd (31–429 mg/kg). Total Ca concentrations are low (< 2 wt% CaO), and calcium carbonate minerals are absent in the studied samples. The occurrence of an important amount of goethite in sample PL_3 is reflected in the high Fe content in this sample (33.6 wt%), compared to the other mine waste samples (2–13 wt% Fe). Additionally, the mine waste samples had a near-neutral pH, with pH values of 7.4, 6.3, 6.6, and 6.2 for samples PL_1, PL_2, PL_3, and PL_4, respectively.

Sequential Extractions

Certified Reference Materials

For quality control of the BCR SE, the use of certified reference materials has increased during the last 15 years but

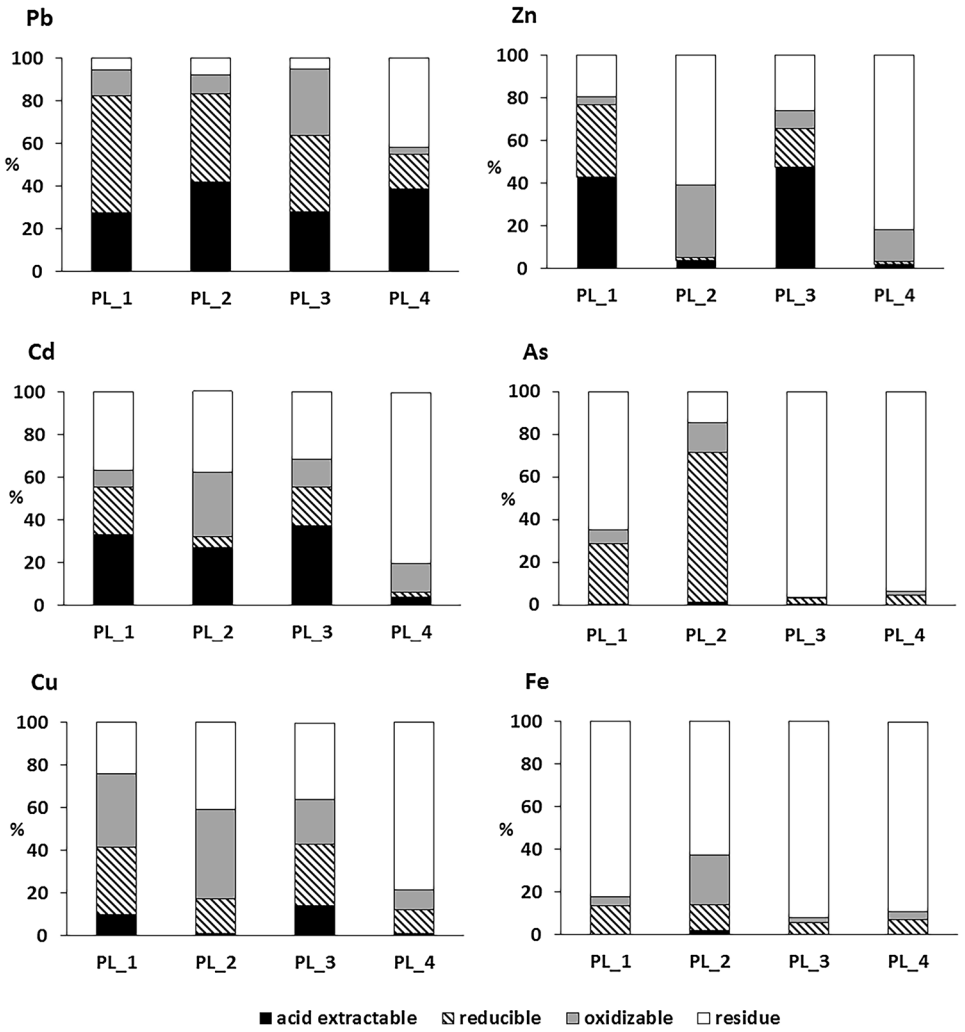

Fig. 2 Distribution of Zn, Pb, Cd, As, Cu, and Fe among the different steps of the BCR SE

is still not a common practice. Two reference materials are made available for the BCR SE procedure, one with certified values for the three extraction steps (BCR 701) and one with indicative values (CRM 483). Both reference materials are sediments with much lower metal(loid) concentrations than normally found in mining waste, and they are also characterized by a composition that is very different from mining waste. The lack of adequate certified reference materials, encompassing the wider range of matrices (and associated metal(loid) concentrations) commonly analyzed with the BCR SE procedure, is an issue that needs urgent attention.

In some studies on mining waste (Supplementary Table S-1), Montana Soil 2710 has also been used as a reference material because of its high Pb and Zn concentrations. Because the samples examined in the present study have high metal(loid) concentrations, this certified reference material (SRM 2710, Montana soil) with high total metal(loid) concentrations was also included in the analyses. No certified values for the BCR SE procedure exist for this reference material but values have been published by several authors (Supplementary Table S-3). The results for the SRM 2710 reference material show a good recovery for all elements (92–108%). When comparing the metal(loid) concentrations in the different extraction steps, the values are in the same range as previously published values. Slightly lower concentrations are measured for Zn in the second extraction step and higher concentrations in the third step. Major elements, such as Fe, Al, and Mn are usually not reported by authors that perform SE. However, the distribution of these elements among different extractions steps can provide information on solid phases (such as Ca-carbonates and Fe(hydr)oxides) that are dissolved by specific reagents.

Mine Waste Samples

Being well aware of the inherent limitations of SEs, the present study considers them as a part of a more integrated approach for material characterization, in which we do not rely solely on SEs. The information obtained from SEs is used in combination with data from the mineralogical

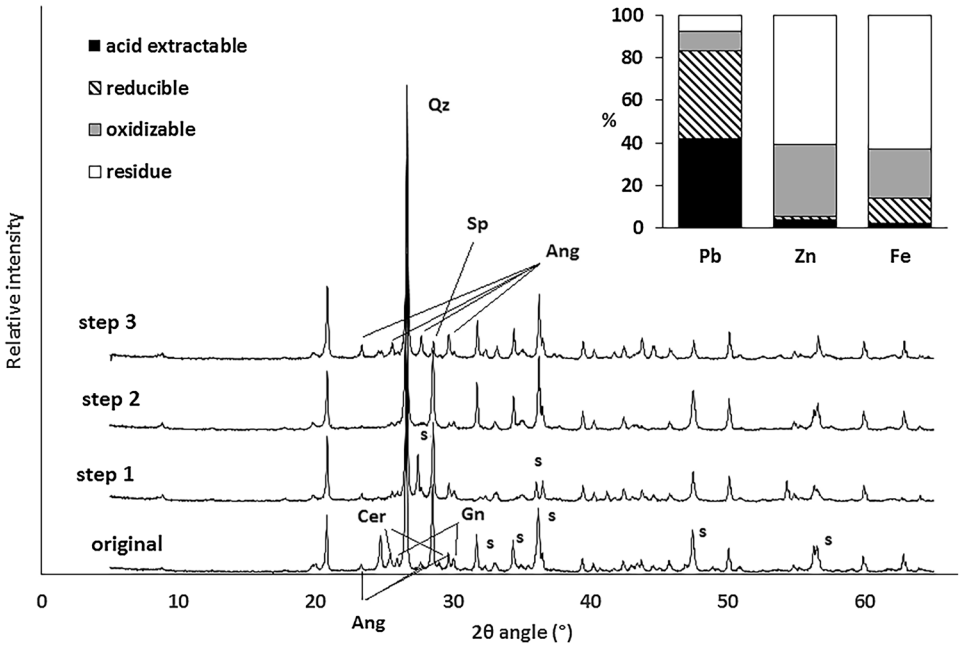

Fig. 3 XRD pattern of the solid phase remaining after the different extraction steps of the BCR SE of sample PL_2. Cerussite (Cer) was dissolved after step 1, anglesite (Ang) only dissolved after step 2 but reappeared after step 3. Sphalerite (Sp) and galena (Gn) partly dissolved in step 3. The internal standard (s) used in step 1 is rutile instead of zincite, which explains the different peaks for the standard

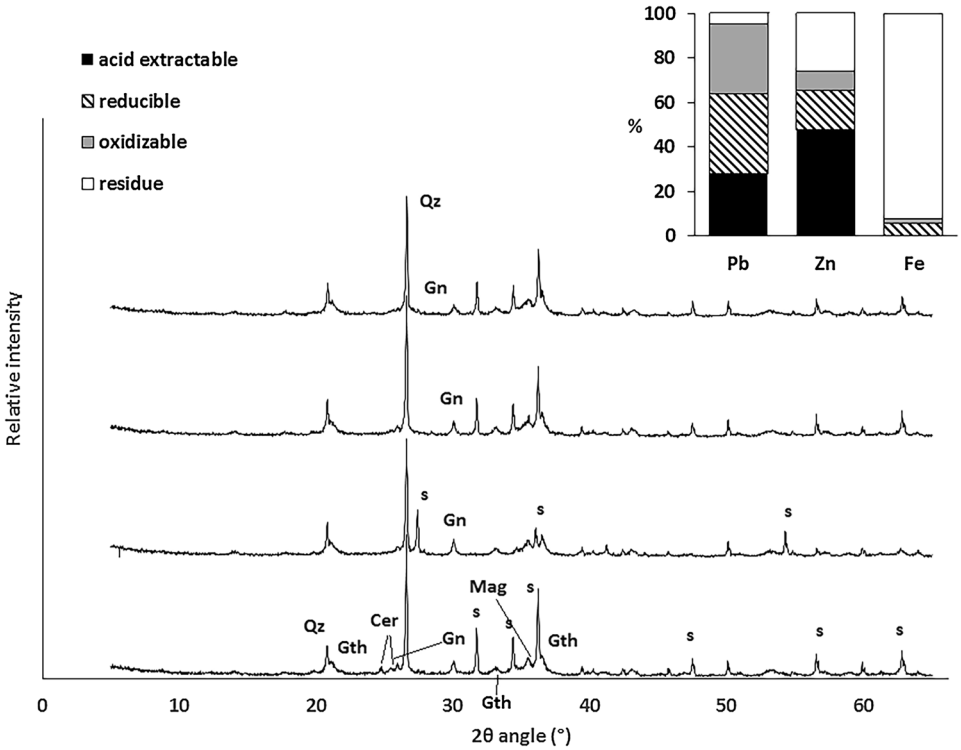

Fig. 4 XRD pattern of the solid phase remaining after the different extraction steps of the BCR SE of sample PL_3. Cerussite (Cer) is dissolved after step 1, while galena (Gn) is partly dissolved after step 3. Goethite (Gth) and magnetite (Mag) are still present after the 3 extraction steps. The internal standard (S) used in step 1 is rutile instead of zincite, which explains the different peaks for the standard

analysis of extracted phases, major element composition, and pH of leachates. As recommended by [34], results are presented in terms of 'operationally defined fractions' (i.e., acid extractable, reducible, oxidizable, and residual fraction). In Figs. 2, 3, and 4, concentrations are described in relative terms, as this makes the comparison between samples easier, but absolute concentrations released in the different steps (presented in Supplementary Table S-6) are also considered when there are significant differences between samples.

The results from the SE, combined with the mineralogical analysis of the residue remaining after each step, indicate that the release of Pb and Zn is mainly controlled by the solubility of Pb/Zn-bearing minerals. Figures 3 and 4 give

the XRD patterns of samples PL_2 and PL_3, after the different extraction steps, together with the SE results for Pb, Zn, and Fe. The quantitative mineralogical composition of the samples, before and after the different steps of the BCR SE, is given in Table 1. Because minerals are dissolved in the different extractions steps, the total mass of the sample decreases, which can be deduced from the increase in relative concentrations of minerals (e.g., quartz) that are not dissolved by the subsequent extractions. In addition, small losses of material during decantation of the liquid and due to violent reactions during the third step can also occur. The information in Table 1 should, therefore, be treated as semi-quantitative information.

Because the pH can have a significant effect on the release of metal(loid)s, the pH of the extracts after steps 1 and 2 were measured. The samples originally all have a near-neutral pH. Sample PL_1 is slightly more alkaline, while PL_2 and PL_4 are slightly more acidic (supplementary Table S-7). The original pH of the acetic acid solution was 2.9. After reacting with the material, a significant increase in pH (0.4–0.8 units) is observed for all the samples due to the dissolution of carbonate phases (cerussite), indicating that the samples have a certain acid neutralization capacity (Supplementary Table S-7).

Lead was mainly recovered in the acid extractable (Step 1) or reducible (Step 2) fraction, except for sample PL_4, where the residual fraction represents the largest fraction of Pb (42%). In the first step of the BCR SE procedure ('acid extractable fraction') 'exchangeable elements' and 'elements bound to carbonates' are released (Fig. 2). Cerussite dissolution occurs at a pH below 6 [35]. As a consequence, cerussite disappears in all investigated samples after the first extraction (Fig. 3), and elevated Pb concentrations are found in the 'acid extractable' fraction. For sample PL_2 and PL_4, a higher release of Pb is measured compared to what would be expected from the dissolution of cerussite alone, indicating that Pb also occurs as readily exchangeable ions.

For sample PL_2, cerussite is dissolved by the acetic acid extraction, whereby a soluble Pb-acetate complex is formed (Step 1):

$$PbCO_3(s) + 2CH_3COOH(aq) \rightarrow (CH_3COO)_2Pb(aq) + CO_2(g) + H_2O. \quad (1)$$

This reaction is not kinetically inhibited, since cerussite completely dissolves after a 16 h extraction time in the first step of the BCR SE procedure.

Anglesite disappeared during the reducing extraction (Step 2). The dissolution of anglesite in the second step of the SE of mine tailing samples was also reported by [10] and [36].

Galena disappears from the sample after the oxidizing extraction (Step 3) (Table 1, Fig. 3), but anglesite (that was previously dissolved during Step 2) reappears (Fig. 3). Oxidative dissolution of galena releases aqueous Pb^{2+} and SO_4^{2-} to the surficial environment and commonly causes the formation of anglesite in acidic environments [37].

$$PbS(s) + 4H_2O_2 \rightarrow PbSO_4(s) + 4H_2O. \quad (2)$$

In theory, $PbSO_4$ will further dissolve with acetate anions (from the ammonium acetate solution used after the H_2O_2 digestion), to give a lead acetate complex in solution [38].

$$PbSO_4(s) + 2CH_3COONH_4(aq) \rightarrow (CH_3COO)_2Pb(aq) + SO_4^{2-} + 2NH_4^+ \quad (3)$$

However, there is probably too much Pb released by the oxidation of galena to be complexed by acetate, which results in the precipitation of non-complexed Pb^{2+} as anglesite.

In kinetic leaching tests of mine tailings at acidic, pH values [39] found that the rapid dissolution of Pb-bearing minerals was followed by the slow precipitation of a sparingly soluble anglesite.

Plumbojarosite and beudantite (sample PL_4) were not dissolved after the first two extractions (Fig. 4), even though the pH of the extraction solution after the second extraction was < 2 (Supplementary Table S-7). Hudson-Edwards et al. [40] performed batch dissolution experiments using a synthetic Pb–As-jarosite (which is a beudantite analog) at pH 2 (20 °C). The dissolution of Pb–As-jarosite produced poorly crystalline solid $PbSO_4$, and Fe^{3+}, and AsO_4^{3-} were released in the aqueous solution.

$$PbFe_3(AsO_4)(SO_4)(OH)_6(s) + 6H^+ \rightarrow PbSO_4(s) + 3Fe^{3+} + AsO_4^{3-} + 6H_2O \quad (4)$$

The different behaviors of beudantite and plumbojarosite in the present study indicate that synthetic samples are not always representative of the complex matrix in which minerals occur in real samples. For instance, shielding by resistant mineral phases, the effect of aging on the reactivity minerals, etc. is not considered when using synthetic samples.

With respect to Zn, a distinction between samples with a rather small (PL_1 and PL_3) and a large (PL_2 and PL_4) residual fraction of Zn can be made (Fig. 2). In the latter samples, only a small fraction of Zn (5% in PL_2 and 3% in PL_4) is released during the first two extraction steps, while in sample PL_1 and PL_3, these two steps represent, respectively, 77% and 66% of the total Zn content, with the largest amount of Zn being released during the acetic acid extraction step (respectively, 43% and 48% of the total Zn content). Sample PL_2 and PL_4 consist of 10.8 wt% and 2.1 wt% ZnS, respectively. The oxidation of sphalerite during the third extraction step is evidenced by the high Zn release during this extraction and by the XRD analyses of the samples after this extraction.

$$ZnS(s) + 4H_2O_2 \rightarrow Zn^{2+} + SO_4^{2-} + 4H_2O \quad (5)$$

If ZnS was to completely dissolve in samples PL_2 and PL_4, respectively 7.2 and 1.4 wt% Zn would be released, which is more than the Zn concentrations measured in the extracts of the 3rd step (respectively, 2.6 and 0.4 wt%) indicating that ZnS did not totally dissolve. This is also shown by the mineralogical composition of the (solid) sample after the third extraction step (Fig. 3, Table 1). In sample PL_4, willemite was partly dissolved after the first extraction step, and disappeared completely after the second extraction (Table 1). The dissolution kinetics of Zns depends on the type of the oxidant used for leaching [41]. H_2O_2 (8.8 mol/l), used in the third step of the BCR SE procedure, does not completely oxidize ZnS, most likely due to slow oxidation kinetics [42].

Both the mineralogical sample composition before and after extractions (Table 1) and the expected element release based on the quantitative mineralogical composition (and assuming that target minerals dissolve completely) show that the dissolution of minerals is not sufficient to explain the release of Zn and Pb. Sorption–desorption of Zn and Pb associated with clay minerals, feldspars, Fe(oxyhydr)oxides, and organic matter should also be taken into account.

The distribution of Cd (Fig. 2) among the different fractions is similar to Zn, except in sample PL_2, for which the acid extractable fraction was more significant (compared to Zn). Although the fractionation of Cd is comparable in samples PL_1, PL_2, and PL_3, the much higher (pseudo-) total content of Cd in sample PL_2 (429 mg/kg) compared to the 3 other samples (31–70 mg/kg) means that an important amount of Cd (168 mg/kg) is easily mobilized from sample PL_2.

The acid extractable fraction of Cu in samples PL_2 and PL_4 (Step 1, 1% of the total concentration), as well as the reducible fraction (Step 2, 11–16%, respectively) is significantly lower compared to samples PL_1 and PL_3 (Fig. 2).

Fe is mainly found in the residual fraction (63 to 91%, Fig. 3), most likely related to the presence of Fe-bearing minerals that are very resistant to acid dissolution. In theory, Fe- and Mn(oxy)(hydr)oxide phases are dissolved during the second step of the BCR SE procedure. However, the solubility of these phases is highly dependent on the crystallinity of the mineral. No clear dissolution of goethite or magnetite is observed in the investigated samples (Table 1).

The relatively high release of As during Step 2 in sample PL_2 (Fig. 3) can be related to the dissolution of (amorphous) Fe-(oxy)(hydr)oxides since As is often strongly bound to Fe-(oxy)(hydr)oxides and a significant correlation between As and Fe distribution (Fig. 3) is observed. However, in absolute terms, a comparable amount of As is released from samples PL_1, PL_2, and PL_4 (Supplementary Table S-6).

Consequences for Metal Recovery and Implications for Health and Environment

The SE indicates that a substantial amount of Pb (55–88%) is easily extracted from the mine waste under acidic conditions (pH < 2). Moreover, a substantial amount of Pb (27- 42%) is present as cerussite in the mine waste, which can easily be recovered by using mild extraction solutions (pH 3–3.8). In view of the high total concentrations of Pb (2.3–15 wt%) in the investigated mine waste samples, this would mean that it is worth considering the valorization of the mine waste, to recover Pb. Based on a recent study, the average Pb and Zn ore grades are 0.44 wt.% and 1.20 wt. %, respectively [43]. The recovery of Zn (total content in the range (2.8–7.0%) is more variable, depending on the sample composition [44]. For samples PL_1 and PL_3, a recovery of respectively 77 and 66% was obtained by the first two extraction steps, while less than 6% of Zn was recovered from samples PL_2 and PL_4. A detailed mapping of the area where the mine waste is stored, with delineation of zones of mine waste with different composition is essential to fully estimate the technical and economic potential of the mine waste as a source of Pb and Zn.

The ancient mining site of Plombières is currently a natural reserve, frequented by walkers and playing children. The mine waste is not fully covered, and ingestion of fine particles (inhalation, hand-to-mouth behavior) is a likely exposure scenario for visitors. Since the pH of the stomach varies between 1.5 and 3.5, the acid extractable fraction (Step 1) from the BCR SE procedure could give a first estimate of released metal(loid)s by stomach acid. Estimates of the relative bioavailability of Pb minerals indicate that cerussite and Mn/Pb oxide are well absorbed by juvenile swines, while galena and anglesite are poorly absorbed [45]. However, other studies consider anglesite as a bioavailable form of Pb that is soluble in stomach acid. The Pb in cerussite readily dissolves on acidic gastric fluids, and is, thus, highly bioaccessible when orally ingested. The oral bioaccessibility of Pb in galena is much lower (less than 10%) [45, 46].

The samples investigated in the present study showed a considerable content of cerussite, pointing to a human health risk when particles are ingested. In mining-affected soils, and in mine waste, metal(loid)s are not necessarily contained in the finest particles, but they can also concentrate in coarser grain size fractions [47]. Bevandić et al. [21] investigated the grain size distributions of 103 samples of mine waste at the Plombières tailings pond. In general, the grain size can be defined as sandy silt to silty sand, where the larger particles relate to the presence of the pyrometallurgical slags in the samples. Especially when Pb is enriched in the clay size fraction of surficial tailings, it could be readily transported by wind, and inhaled, ingested, or deposited

as dust [48]. The study of [21] indicated that the silt fraction was dominant in the mine waste samples of Plombières. The partitioning of metal(loid)s among different grain size fractions was not within the scope of the present study, but future research with respect to human health risk assessment in the Plombières mining area should focus on the exposure to Pb, Zn, Cd, and As, taking into account the chemical and mineralogical composition of different grain size fractions. Additionally, runoff and erosion can also contribute to the dispersal of mine waste particles.

Some authors state that the formation of plumbojarosite in contaminated soils can reduce the relative bioaccessibility of Pb [49] and that beudantite can efficiently immobilize As and Pb, and is stable under acidic and oxidizing conditions [29]. However, other authors [40] stress that further research is necessary with respect to the longer-term (> 1 year) stability of minerals such as beudantite and plumbojarosite. Due to the considerable amount of Pb that is found as cerussite, the high mobility of Pb seems to be the main concern at the moment. Currently, the mine waste has a near-neutral pH. However, considering the longer term, if acidification occurs, the mine waste may also release Zn, Cd, and As into the environment. For a long-term risk assessment, the role of microbial processes on the release of metal(loid)s should be taken into account. The SE shows that reducing conditions (Step 2) release Pb from all samples and As from samples PL_1 and PL_2 (Fig. 3). However, this extraction is performed at acidic pH values and does not take into account microbially driven reactions, which, at neutral, pH can result in the reduction of Fe(III) and As(V), and the partial mobilization of As [50].

Conclusions

A variety of Pb/Zn-bearing minerals are present in the mining and metallurgical waste of Plombières, including primary sulfides (galena and sphalerite), as well as secondary minerals such as willemite, cerussite, anglesite, and plumbojarosite. Different methods, providing complementary information, were applied to determine the (pseudo-) total element composition of the mine waste samples. The concentrations of As (one sample), Cd, and Cu were below the detection limit of XRF and could only be determined with the $LiBO_2$ and AR methods. However, the $LiBO_2$ fusion method could not completely dissolve the samples, due to the presence of refractory minerals and slag particles and, thus, only provides a quantification of pseudo-total element concentrations. Moreover, some elements such as Cd and As were (partly) volatilized during the $LiBO_2$ fusion, yielding higher concentrations of these elements by the AR method, despite the higher insoluble residue left after the AR digestion.

Sequential extraction results, in combination with the mineralogical data obtained after the different extraction steps, indicate which minerals dissolve and are responsible for the release of metal(loid)s in each extraction step. However, precipitation of secondary minerals (e.g., anglesite), the incomplete dissolution of some minerals (e.g., galena, sphalerite), and (de)sorption reactions should also be considered. Quantitative XRD analysis allowed for the better evaluation of the incomplete dissolution of some minerals, improving the interpretation of the SE results.

Although the BCR SE has been designed for soils and sediments, it proved to be useful for the characterization of mine waste samples. For a thorough understanding of processes that control the release or sequestration of metal(loid)s in mine waste, a detailed chemical and mineralogical characterization of the material is important. It allows to better predict the reactivity of the mining waste, for example, upon interaction with water, acid rain, digestive fluids, and/or when it ends up in an oxidizing or reducing environment. This is not only essential information for human health and environmental risk assessments but is also crucial information to evaluate the potential of resource recovery and recycling. The present study showed that Pb was the element with the highest potential for recovery from the mining waste, and that Pb is also the element that poses the highest environmental and human health risks, especially because cerussite is present in the mine waste.

Finally, we recommend creating a certified reference material for the BCR SE, with a composition that better approximates the composition of mining and metallurgical waste. Although 'mining and metallurgical waste' includes a range of materials with different compositions, at least the high total concentrations of this type of material, as well as the presence of components with a low solubility towards the reagents of the BCR SE could be taken into account.

Supplementary Information The online version contains supplementary material available at https://doi.org/10.1007/s40831-021-00455-y.

Acknowledgements We are grateful to Dr. Elvira Vassilieva for carrying out the ICP-OES analyses and to Wienerberger NV—Central Laboratory Beerse for the XRF analyses. We also thank D. Bonni of the 'L'Agence de Développement Local de Lontzen, Plombières et Welkenraedt' for his support and valuable information on the ancient mining site, and T. Wimmer and J. Drooghaag for the permission to take samples from the historic mining site of Plombières. The SULTAN project has received funding from the European Union's EU Framework Programme for Research and Innovation Horizon 2020 under Grant Agreement No 812580 (SULTAN, https://etn-sultan.eu).

Declarations

Conflict of interest On behalf of all authors, the corresponding author states that there is no conflict of interest.

References

1. Eurostat (2018) Waste statistics. https://ec.europa.eu/eurostat/statistics-explained/index.php/Waste_statistics#Total_waste_generation
2. Gutiérrez M, Mickus K, Mar Camacho L (2016) Abandoned Pb-Zn mining wastes and their mobility as proxy to toxicity: a review. Sci Total Environ 565:392–400. https://doi.org/10.1016/j.scitotenv.2016.04.143
3. Jabłońska-Czapla M, Nocoń K, Szopa S et al (2016) Impact of the Pb and Zn ore mining industry on the pollution of the Biała Przemsza River. Poland Environ Monit Assess 188:262. https://doi.org/10.1007/s10661-016-5233-3
4. Hudson-Edwards KA, Macklin MG, Finlayson R, Passmore DG (1999) Medieval lead pollution in the River Ouse at York, England. J Archaeol Sci 26:809–819. https://doi.org/10.1006/jasc.1998.0357
5. BRGM (2001) Management of mining, quarrying and ore-processing waste in the European Union, 79 p., 7 Figs., 17 Tables, 7 annexes, 1 CD-ROM (Collected data)
6. European Commission (2019) Study supporting the elaboration of guidance on best practices in the extractive waste management plans Final Report Eco Efficiency Consulting and Engineering Ltd.in collaboration with WEFalck, Pöyry Finland Oy, Botond Kertész & CRS Ingenería, 126 pp.
7. Zhang X, Yang L, L, Y, et al (2012) Impacts of lead/zinc mining and smelting on the environment and human health in China. Environ Monit Assess 184:2261–2273. https://doi.org/10.1007/s10661-011-2115-6
8. Rodgers KJ, Hursthouse A, Cuthbert S (2015) The potential of sequential extraction in the characterisation and management of wastes from steel processing: a prospective review. Int J Environ Res Public Health 12:11724–11755. https://doi.org/10.3390/ijerph120911724
9. Calmano W, Mangold S, Welter E (2001) An XAFS investigation of the artefacts caused by sequential extraction analyses of Pb-contaminated soils. Fresenius J Anal Chem 371:823–830. https://doi.org/10.1007/s00216-001-1106-9
10. Cappuyns V, Swennen R, Niclaes M (2007) Application of the BCR sequential extraction scheme to dredged pond sediments contaminated by Pb-Zn mining: a combined geochemical and mineralogical approach. J Geochem Expl 93(2):78–90. https://doi.org/10.1016/j.gexplo.2006.10.001
11. Clevenger TE (1990) Use of sequential extraction to evaluate the heavy metals in mining wastes. Water Air Soil Pollut 50:241–254. https://doi.org/10.1007/BF00280626
12. Spanka M, Mansfeldt T, Bialucha R (2018) Sequential extraction of chromium, molybdenum, and vanadium in basic oxygen furnace slags. Environ Sci Pollut Res 25:23082–23090. https://doi.org/10.1007/s11356-018-2361-z
13. Ryan PC, Hillier S, Wall AJ (2008) Stepwise effects of the BCR sequential chemical extraction procedure on dissolution and metal release from common ferromagnesian clay minerals: a combined solution chemistry and X-ray powder diffraction study. Sci Total Environ 407:603–614. https://doi.org/10.1016/j.scitotenv.2008.09.019
14. Dejonghe L (1998) Zinc-lead deposits of Belgium. Ore Geol Rev 12:329–354. https://doi.org/10.1016/S0169-1368(98)00007-9
15. Rauret G, Lopez-Sanchez JF, Sahuquillo A, Rubio R, Davidson C, Ure A, Quevauviller P (1999) Improvement of the BCR three step sequential extraction procedure prior to the certification of new sediment and soil reference materials. J Environ Monit 1:57–61. https://doi.org/10.1039/A807854H
16. Blondieau M, Polrot F (2011) Les travaux miniers de Schimper, siège sud de la mine du Bleyberg (Plombières, Belgique):Plomb, zinc mais aussi argent: Histoire, minéralisations, production d'argent, impact dans le paysage. Geological Survey of Belgium Professional Paper 310, 57 pp, ISBN 0378-0902
17. Helser J, Vassilieva E, Cappuyns V (2022) Environmental and human health risk assessment of sulfidic mine waste: bioaccessibility, leaching and mineralogy. J Hazard Mater. https://doi.org/10.1016/j.jhazmat.2021.127313
18. Giels M, Iacobescu RI, Cappuyns V, Pontikes Y, Elsen J (2019) Understanding the leaching behavior of inorganic polymer made of iron rich slags. J Clean Prod. https://doi.org/10.1016/j.jclepro.2019.117736
19. Bergmann J, Friedel P, Kleeberg R (1998) BGMN—A new fundamental parameter based Rietveld program for laboratory X-ray sources, its use in quantitative analysis and structure investigations. CPD Newsletter, Commission of Powder Diffraction. Int Union Crystallogr 20:5–8
20. Cappuyns V, Van Campen A, Helser J (2021) Antimony leaching from soils and mine waste from the Mau Due antimony mine. North-Vietnam J Geoch Expl 220:106663. https://doi.org/10.1016/j.gexplo.2020.106663
21. Bevandić S, Blannin R, Vander Auwera J, Delmelle N, Caterina D, Nguyen F, Muchez P (2021) Geochemical and mineralogical characterisation of historic Zn–Pb mine waste, Plombières, East Belgium. Minerals 11:28. https://doi.org/10.3390/min11010028
22. Duval DJ, Risbud SH, Shackelford JF (2008) Mullite. In: Shackelford J.F., Doremus R.H. (eds) Ceramic and glass materials. Springer, Boston. https://doi.org/10.1007/978-0-387-73362-3_2
23. Keim M, Markl G (2015) Weathering of galena: mineralogical processes, hydrogeochemical fluid path modeling, and estimation of the growth rate of pyromorphite. Am Mineral 100(7):1584–1594. https://doi.org/10.2138/am-2015-5183
24. Li X, Azimzadeh B, Martinez CE, McBride MB (2021) Pb mineral precipitation in solutions of sulfate, carbonate and phosphate: measured and modeled Pb solubility and Pb^{2+} activity. Minerals 11:620. https://doi.org/10.3390/min11060620
25. Hemphill CP, Ruby MV, Beck BD, Davis A, Bergstrom PD (1991) The bioavailability of lead in mining wastes: physical/chemical considerations. Chem Speciation Bioavail 3(3–4):135–148. https://doi.org/10.1080/09542299.1991.11083165
26. Jambor J, Nordtrom D, Alpers C (2000) Metal-sulfate salts from sulfide mineral oxidation. Rev Mineral Geoch 40:302–350. https://doi.org/10.2138/rmg.2000.40.6
27. Li M, Peng B, Chai L-Y, Peng N, Xie X, Yan H (2013) Technological mineralogy and environmental activity of zinc leaching residue form zinc hydrometallurgical process. Trans Nonferr Metals Soc China 23:1480–1488. https://doi.org/10.1016/S1003-6326(13)62620-5
28. Nieto JM, Capitán MA, Sáez R, Almodóvar GR (2003) Beudantite: a natural sink for As and Pb in sulphide oxidation processes. Appl Earth Sci 112(3):293–296. https://doi.org/10.1179/037174503225003134
29. Courtin-Nomade A, Neel C, Bril H, Davranche M (2002) Trapping and mobilisation of arsenic and lead in former mine tailings—environmental conditions effects. Bull Société Géologique Fr 173:479–485. https://doi.org/10.2113/173.5.479
30. Welch SA, Christy AG, Kirste D, Beavis SG, Beavis F (2007) Jarosite dissolution I—trace cation flux in acid sulfate soils. Chem Geol 245:183–197. https://doi.org/10.1016/j.chemgeo.2008.06.010

31. Frost RL, Palmer SJ, Spratt HJ, Martens WN (2011) The molecular structure of the mineral beudantite $PbFe_3(AsO_4, SO_4)2(OH)6$—implications for arsenic accumulation and removal. J Mol Struct 988:52–58. https://doi.org/10.1016/j.molstruc.2010.12.002
32. Helser J, Cappuyns V (2021) Trace elements leaching from Pb-Zn mine waste (Plombières, Belgium) and environmental implications. J Geoch Expl 220:106659. https://doi.org/10.1016/j.gexplo.2020.106659
33. Zhang Y, Evans J, Yang S (2011) Corrected values for boiling points and enthalpies of vaporization of elements in handbooks. J Chem Eng Data 56(2):328–337. https://doi.org/10.1021/je1011086
34. Bacon JR, Davidson CM (2008) Is there a future for sequential chemical extraction? Analyst 133:25–46. https://doi.org/10.1039/B711896A
35. Krauskopf KB, Bird DK (1994) Introduction to geochemistry, 3rd edn. McGraw-Hill International Editions, New York
36. Fonseca EC, Martin H (1986) The selective extraction of Pb and Zn in selected mineral and soil samples, application in geochemical exploration (Portugal). J Geochem Explor 26:231–248
37. Bao Z, Al T, Couillard M, Poirier G, Bain J, Shrimpton HK, Finfrock YZ, Lanzirotta A, Paktunc D, Saurette E et al (2021) A crossscale investigation of galena oxidation and controls on mobilization of lead in mine waste rock. J Hazard Mater 412:125130. https://doi.org/10.1016/j.jhazmat.2021.125130
38. Aydoğan S, Aras A, Uçar G, Erdemoğlu M (2007) Dissolution kinetics of galena in acetic acid solutions with hydrogen peroxide. Hydrometall 89:189–195. https://doi.org/10.1016/j.hydromet.2007.07.004
39. Lee PK, Kang MJ, Jo HY et al (2012) Sequential extraction and leaching characteristics of heavy metals in abandoned tungsten mine tailings sediments. Environ Earth Sci 66:1909–1923. https://doi.org/10.1007/s12665-011-1415-z
40. Hudson-Edwards KA (2019) Uptake and release of arsenic and antimony in alunite-jarosite and beudantite group minerals. Am Mineral 104:633–640. https://doi.org/10.2138/am-2019-6591
41. Picazo-Rodríguez NG, Soria-Aguilar MdJ, Martínez-Luévanos A, Almaguer-Guzmán I, Chaidez-Félix J, Carrillo-Pedroza FR (2020) Direct acid leaching of sphalerite: an approach comparative and kinetics analysis. Minerals 10:359. https://doi.org/10.3390/min10040359
42. Chopard A, Benzaazoua M, Plante B, Bouzahzah H, Marion P (2015) Kinetic tests to evaluate the relative oxidation rates of various sulfides and sulfosalts. In: Proceedings of the 10th ICARD Conference on Acid Rock Drainage, and IMWA, Santiago, Chile, 21–24 April 2015
43. Mudd MG, Jowitt SM, Werner TT (2017) The world's lead-zinc mineral resources: scarcity, data, issues and opportunities. Ore Geol Rev 80:1160–1190. https://doi.org/10.1016/j.oregeorev.2016.08.010
44. Bevandić S, Xanthopoulos P, Muchez P (2021) Chemical leaching of sulfidic mining waste, Plombières tailings pond, eastern Belgium: insights from a mineralogical approach. J Sustain Metall 10:20. https://doi.org/10.1007/s40831-021-00445-0
45. Casteel SW, Weis CP, Henningsen GM, Brattin WJ (2006) Estimation of relative bioavailability of lead in soil and soil-like materials using young swine. Environ Health Perspect 114:1162–1171. https://doi.org/10.1289/ehp.8852
46. Bosso ST, Enzweiler J (2008) Bioaccessible lead in soils, slag, and mine wastes from abandoned mining district in Brazil. Environ Geochem Health 30:219–229. https://doi.org/10.1007/s10653-007-9110-4
47. Hoshino M, Zhang M, Suzuki M, Tsukimura K, Ohta M (2020) Characterization of Pb-bearing minerals in polluted soils from closed mine sites. Water Air Soil Pollut 231:176. https://doi.org/10.1007/s11270-020-04548-4
48. Hayes SM, O'Day PA, Webb SM, Maier RM, Chorover J (2011) Changes in zinc speciation with mine tailings acidification in a semiarid weathering environment. Environ Sci Technol 45(17):7166–7172. https://doi.org/10.1021/es201006b
49. Karna RR, Noerpel MR, Nelson C, Elek B, Herbin-Davis K, Diamond G, Bradham K, Thomas DJ, Scheckel KG (2021) Bioavailable soil Pb minimized by in situ transformation to plumbojarosite. Proc Nat Acad Sci 118(3):e2020315117. https://doi.org/10.1073/pnas.2020315117
50. Smith AML, Dubbin WE, Wright K, Hudson-Edwards KA (2006) Dissolution of lead- and leadarsenic jarosites at pH 2 and 8: insights from batch experiments. Chem Geol 229:344–361. https://doi.org/10.1016/j.chemgeo.2005.11.006